

# THE REALISTIC VERSUS THE SPHERICAL HEAD MODEL IN EEG DIPOLE SOURCE ANALYSIS IN THE PRESENCE OF NOISE

Bart Vanrumste<sup>1,2</sup>, Gert Van Hoey<sup>1,2</sup>, Rik Van de Walle<sup>1</sup>,  
Peter Van Hese<sup>1,2</sup>, Michel. D'Havé<sup>2</sup>, Paul Boon<sup>2</sup>, and Ignace Lemahieu<sup>1</sup>

<sup>1</sup>Department of Electronics and Information Systems, Ghent University  
Sint-Pietersnieuwstraat 41, B-9000 Ghent, Belgium

<sup>2</sup> Epilepsy Monitoring Unit, Department of Neurology, Ghent University Hospital  
De Pintelaan 185, B-9000 Ghent, Belgium

E-mail: bart.vanrumste@elis.rug.ac.be, Tel. +32-9-240.43.85, Fax. +32-9-240.49.71

## ABSTRACT

The performance of the three-shell spherical head model versus the performance of the realistic head model is investigated when solving the inverse problem with a single dipole, in the presence of noise. This is evaluated by inspecting the average dipole location error when applying a spherical and a realistic head model, for 1000 noisy scalp potentials, originating from the same test dipole and having the same noise level. The location errors are obtained utilizing a local linearization, which is validated with a Monte Carlo simulation. For 27 electrodes, an EEG epoch of one time sample and spatially white Gaussian noise we found that the importance of the realistic head model over the spherical head model reduces by increasing the noise level. **Keywords:** EEG dipole source analysis; Gaussian noise; realistic head

## Report Documentation Page

<b>Report Date</b> 25 Oct 2001	<b>Report Type</b> N/A	<b>Dates Covered (from... to)</b> -
<b>Title and Subtitle</b> The Realistic Versis the Spherical Head Model in EEG Dipole Source Analysis in The Presence of Noise		<b>Contract Number</b>
		<b>Grant Number</b>
		<b>Program Element Number</b>
<b>Author(s)</b>		<b>Project Number</b>
		<b>Task Number</b>
		<b>Work Unit Number</b>
<b>Performing Organization Name(s) and Address(es)</b> Department of Electronics and Information Systems Ghent University Sint-Pietersnieuwstraat 41, B-9000 Ghent Belgium		<b>Performing Organization Report Number</b>
<b>Sponsoring/Monitoring Agency Name(s) and Address(es)</b> US Army Research, Development & Standardization Group (UK) PSC 802 Box 15 FPO AE 09499-1500		<b>Sponsor/Monitor's Acronym(s)</b>
		<b>Sponsor/Monitor's Report Number(s)</b>
<b>Distribution/Availability Statement</b> Approved for public release, distribution unlimited		
<b>Supplementary Notes</b> Papers from 23rd Annual International Conference of the IEEE Engineering in Medicine and Biology Society, October 25-28, 2001, held in Istanbul, Turkey. See also ADM001351 for entire conference on cd-rom.		
<b>Abstract</b>		
<b>Subject Terms</b>		
<b>Report Classification</b> unclassified	<b>Classification of this page</b> unclassified	
<b>Classification of Abstract</b> unclassified	<b>Limitation of Abstract</b> UU	
<b>Number of Pages</b> 4		

The spherical head model is constructed as follows. Through the 27 electrode nodes located at the scalp surface, used in the finite difference volume conductor model, a best-fitting sphere is constructed with a radius  $R$ . A radial projection of the electrodes on the surface of the sphere is performed to obtain the electrode coordinates on the spherical head model. The radii of the outer shell of the scalp, skull and brain are  $R$ ,  $\frac{85}{92}R$  and  $\frac{80}{92}R$ , respectively.

When applying the spherical head model, the electrode positions need to be obtained to construct the best-fitting sphere. In contrast, when applying a realistic head model, the segmented MR-image needs to be constructed, the electrode positions need to be obtained and the numerical pre-processing needs to be performed. It is clear that the latter is more demanding.

## 2.2. The inverse problem

The EEG presented at the input of the inverse solver, with  $l$  electrodes (27) and for a single time instant can be given by  $\mathbf{V}_{in} \in \mathbb{R}^{l \times 1}$ . The three location parameters and the three components of the dipole are obtained by finding the global minimum of the residual energy (RE):

$$RE = \|\mathbf{V}_{in} - \mathbf{V}_{model}\|^2,$$

with  $\mathbf{V}_{model} \in \mathbb{R}^{l \times 1}$  the electrode potentials obtained by the forward evaluation in the inverse problem and  $\|\cdot\|$  the  $L_2$  norm.

The RE indicates the fraction of energy, which cannot be modeled by the dipole. The Nelder-Mead simplex method is used to find the optimal position  $\mathbf{r}_{opt}$ . For each dipole position the optimal components  $\mathbf{d}_{opt}$  are found in the least-squares sense.

## 2.3. The construction of $R$

For a given test dipole, with dipole position  $\mathbf{r}_0$  and components  $\mathbf{d}_0$ , the forward problem is solved in a realistic head model, yielding a set of average referenced scalp potentials. From these noiseless set of potentials, noisy sets of potentials are generated by adding noise values to each of the potentials. These noise values can be described as a Gaussian with zero mean. Using the noiseless forward calculated potentials in the realistic head model, the inverse problem is solved in a spherical head model yielding dipole position  $\mathbf{r}_{sphere}$  and components  $\mathbf{d}_{sphere}$ . A local linearization of the forward problem as presented in [10, 11] with the spherical head model at these dipole parameters is then performed. This gives us the opportunity to solve for the deviations of the dipole positions  $\Delta \mathbf{r}_{noise, i}^{sphere}$  as a function of the noise values at the electrodes. These results are obtained with a matrix multiplication, which is faster than solving the inverse problem iteratively. Furthermore,  $i = 1 \dots 1000$  corresponds with one of the 1000 noisy potential sets with noise values coming from the same distribution having a given standard deviation corresponding with a given noise level. The location error due to noise and due to the spherical head model then becomes:

$r_i^{sphere} = \|\Delta \mathbf{r}_{noise, i}^{sphere} + \mathbf{r}_{sphere} - \mathbf{r}_0\|$ , where  $\|\cdot\|$  is the Euclidian norm. For a 1000 noisy potentials sets, we obtain the average location error  $E(r_i^{sphere})$ . Next we calculate the deviation of the dipole coordinated  $r_i^{real}$ , utilizing a realistic head model and due to noise. Notice that we assume that the inverse solver, applying the realistic head model, is an unbiased estimator. A local linearization of the forward problem with the realistic head model at the test dipole position  $\mathbf{r}_0$  and orientation  $\mathbf{d}_0$ , is then performed. The location error due to noise then becomes:  $r_i^{real} = \|\Delta \mathbf{r}_{noise, i}^{real}\|$ ,

where  $\Delta \mathbf{r}_{noise, i}^{real}$  is the deviation from the test dipole position for given noise values. For the same 1000 noisy potential sets as in the spherical head model case we then calculate the average location error,  $E(r_i^{real})$ .

When  $E(r_i^{sphere})$  is much larger than  $E(r_i^{real})$ , for a certain noise level, then it is worthwhile using the more efficient demanding realistic head model instead of the spherical head model. On the other hand, when  $E(r_i^{sphere})$  has about the same value as  $E(r_i^{real})$ , then it does not matter whether a realistic or a spherical head is used. Therefore, the difference between the two average location errors  $R = E(r_i^{sphere}) - E(r_i^{real})$  is introduced. We suggest that a  $R$  smaller than 5 mm indicates that for a given dipole and for a given noise level both models, the spherical and the realistic head model perform equally. On the other hand when  $R$  is larger than 5 mm for a given dipole and for a given noise level we argue that in this case the realistic head model performs better than the spherical model.

## 2.4. Validation of the linearization

A first simulation is carried out to evaluate the local linearization for one test dipole. We have calculated  $E(r_i^{sphere})$  and  $E(r_i^{real})$  for a number of noise levels and for 1000 noisy potential distributions, utilizing the local linearization. On the other hand we have calculated, for the same noisy scalp potentials, the inverse problem in a spherical and realistic head model. This approach is often called a Monte-Carlo simulation. The average location errors are derived and compared with the ones found utilizing the local linearization.

## 2.5. $R$ for 27 electrodes and Gaussian noise

In the second simulation, 427 test dipole positions, located in a coronal slice containing the vertex electrode 'Cz', are used. For each test position a dipole along the x-, y-, and z-axis is generated yielding 1281 test dipoles. The x-axis is oriented from the left towards the right ear, the y-axis is oriented from the back of the head towards the nose, and the z-axis is oriented from the bottom of the head towards the vertex electrode 'Cz'.

Further more the grand average over 1281 dipoles of  $R$ , represented by  $A(\Delta R)$ , is also given as a function of the noise level. Notice that  $A(\cdot)$  calculate the average for all test dipoles while  $E(\cdot)$  calculates the average for all noisy potential distributions associated with one test dipole.

To have a more quantitative measure for a given noise level, the number of test dipoles are counted which have a  $R$  larger than the chosen 5 mm. This gives us the opportunity to investigate, for a given noise level and for a large number of test dipoles, whether it is still worthwhile utilizing the more computational demanding realistic head model, instead of the spherical head model.

# 3. RESULTS

## 3.1. Validation of the local linearization

The results obtained with the local linearization are validated utilizing Monte Carlo simulations for one test dipole. The solid line in figure 1 presents the average dipole location error  $E(r_i^{real})$  obtained with a local linearization of the forward problem with the realistic head model, instead of the spherical head model.

theadhdals, cis(on)KHn]2IPk]3]32K

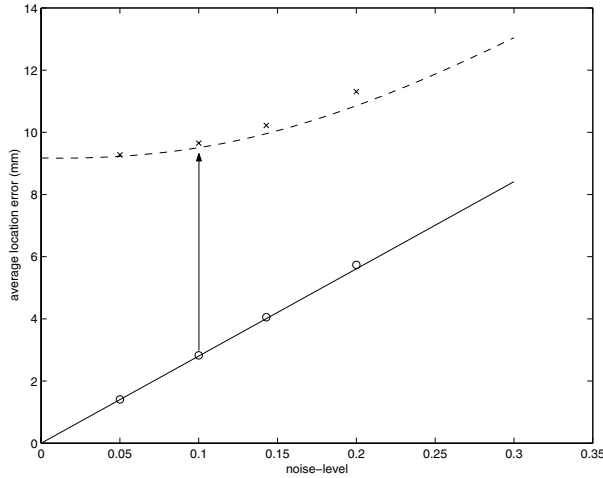


Figure 1. The solid line (-) and the dashed line (- -), depict the average dipole location error as a function of the noise level obtained with the local linearization of the forward function when utilizing a realistic and spherical head model, respectively. The (o) and (x) present the average dipole location errors obtained with a Monte-Carlo simulation, for noise levels 0.2, 0.14, 0.1, and 0.05, utilizing the realistic and spherical head model, respectively. The difference between the average location error obtained with the spherical and realistic head model or  $R$  for the noise level of 0.1 is illustrated with the arrow.

an average location error. The 'o' depicts the average location error obtained from a Monte-Carlo simulation for the noise levels 0.05, 0.1, 0.14 and 0.2, utilizing the realistic head model. The 'x' depicts the average location error obtained from a Monte-Carlo simulation, utilizing a spherical model. One can notice that the average location errors obtained with the Monte-Carlo simulation correspond well with the values obtained through local linearization, and this even for larger noise levels. The  $R = E(r_i^{sphere}) - E(r_i^{real})$ , for noise level 0.1, is marked with the arrow in figure 1. It can also be observed that by increasing the noise level the value of  $R$  decreases.

### 3.2. $R$ for 27 electrodes and Gaussian noise

The first, second, third and fourth row in figure 2 present the value  $R = E(r_i^{sphere}) - E(r_i^{real})$  for a noise level equal to 0, 0.05, 0.1 and 0.2, respectively as a function of the dipole position. The dipole orientation is along the x-axis. A contour with  $R$  equal to 5 mm is also given. For noise level zero  $R$  equals  $E(r_i^{sphere})$ . By increasing the noise level, the  $R$  values decrease for all test dipoles. Hence the areas where  $R$  is larger than 5 mm decrease when increasing the noise level.

The grand average over all the test dipole positions of  $R$  is presented in the column marked with  $A(\Delta R)$  in table 1. It can be observed that by increasing the noise level the grand average of  $R$ , decreases from 5.5 mm to 1.8 mm.

In table 1, the percentage of  $R$  values larger than 5 mm are also given, for the applied noise levels. Notice that 60% of the test dipole have a  $R$  larger than 5 mm for the noise-less case. Evoked potentials and epileptic spikes coming from the same focal source are often averaged, to reduce the background EEG. For the averaged spikes the noise level is typical situated around 0.1. For this noise level 13.4% of the test dipoles have a  $R$  larger than 5 mm. This number decreases

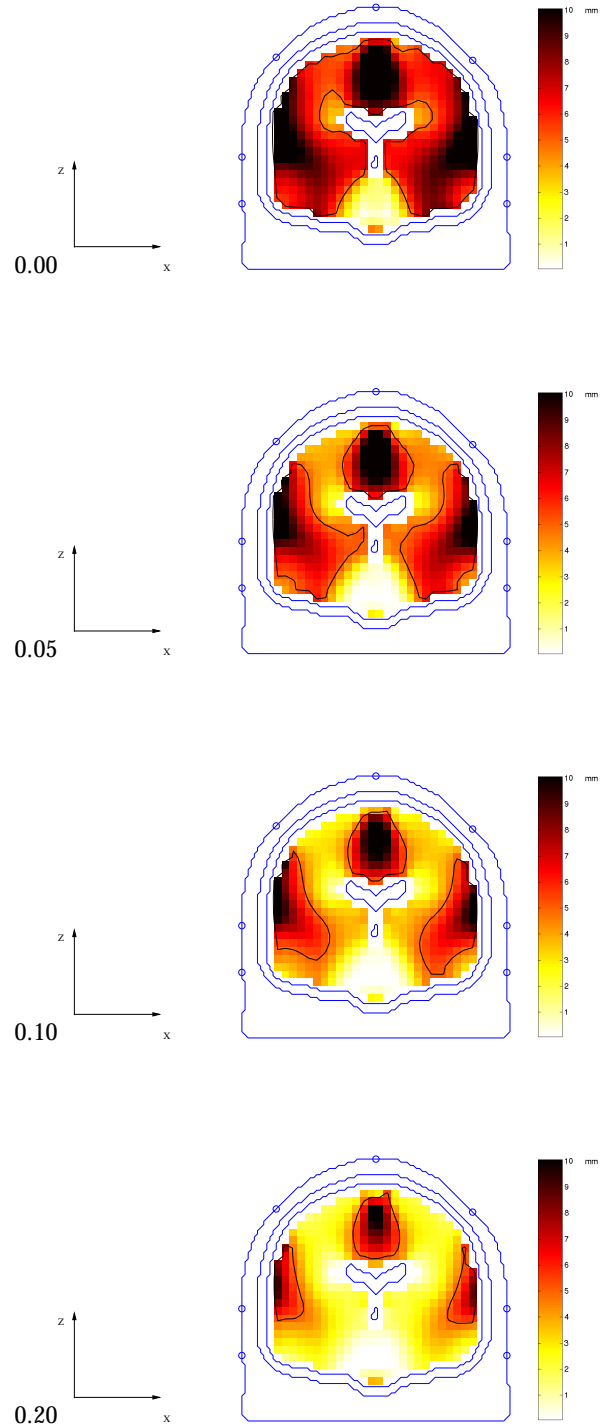


Figure 2. The first, second, third and fourth row illustrate  $R = E(r_i^{sphere}) - E(r_i^{real})$  for noise levels equal to 0, 0.05, 0.1 and 0.2, respectively. A contour with  $R$  equal to 5 mm is also given. The configuration with 27 electrodes and Gaussian noise is used. The results for dipoles oriented along the x-axis are depicted.

Table 1. The grand average over the 1281 test dipole for  $R_i$  is presented. Further more, the relative number of test dipoles yielding a  $R_i$  larger than 5 mm, is also given. The noise levels 0, 0.05, 0.1 and 0.2 are considered. 27 electrodes, and Gaussian noise is applied.

noise level	SNR	A( $\Delta R$ )(mm)	#( $R_i > 5$ mm)(%)
0.0	$\infty$	5.5	60.0
0.05	20	4.0	25.5
0.1	10	3.1	13.4
0.2	5	1.8	7.6

to 7.6% for a noise level of 0.2, which corresponds with an unaveraged epileptic spike. The higher the noise level, the less important becomes the usage of the realistic head model over the spherical head model.

#### 4. CONCLUSION

The aim of this paper was to evaluate the performance of the three-shell spherical head model versus the performance of the realistic head model, in solving the inverse problem with a single dipole in the presence of noise. In our simulations, the average location errors  $E(r_i^{sphere})$  and  $E(r_i^{real})$  are obtained through a local linearization. As control we found for one dipole that the values of  $E(r_i^{sphere})$  and  $E(r_i^{real})$  obtained through local linearization are in good agreement with the ones obtained when utilizing a Monte Carlo approach. When utilizing 27 electrodes, an epoch of one time sample and Gaussian noise, it was found that by increasing the noise level from 0 to 0.2, that the grand average over all the test dipoles of  $R_i$  decreased from 5.5mm to 1.8mm, respectively. For a noise level of 0.1, corresponding with an averaged epileptic spike, 13.4% of the test dipoles have a  $R_i$  larger than 5mm. For a noise level of 0.2, corresponding with an unaveraged epileptic spike, less than 10 % of the test dipoles have a  $R_i$  larger than 5mm. The importance of the realistic head model over the spherical head model reduces by increasing the noise level.

#### ACKNOWLEDGMENT

Bart Vanrumste and Paul Boon are supported by grants from the Fund for Research of the Ghent University, Belgium (Bijzonder Onderzoeksfonds RUG, 01104495 - 011A0996 - 01105399 - 011D0996). Rik Van de Walle is a post-doctoral Fellow of the Fund for Scientific Research Flanders, Belgium.

#### REFERENCES

- [1] P. Boon and M. D'Havé, "Interictal and ictal dipole modelling in patients with refractory partial epilepsy," *Acta Neurologica Scandinavica*, vol. 92, pp. 7–18, 1995.
- [2] B. Roth, A. Gorbach, and S. Sato, "How well does a three-shell model predict positions of dipoles in a realistically shaped head?," *Electroencephalography and Clinical Neurophysiology*, vol. 87, pp. 175–184, 1993.
- [3] B. Yvert, O. Bertrand, M. Thévenet, J. F. Echallier, and J. Pernier, "A systematic evaluation of the spherical model accuracy in EEG dipole localization," *Electroencephalography and Clinical Neurophysiology*, vol. 102, pp. 452–459, May 1997.
- [4] J. C. Mosher, M. E. Spencer, R. M. Leahy, and P. S. Lewis, "Error bounds for EEG and MEG dipole source localization," *Electroencephalography and Clinical Neurophysiology*, vol. 86, pp. 303–321, 1993.

- [5] G. Van Hoey, B. Vanrumste, M. D'Havé, R. Van de Walle, I. Lemahieu, and P. Boon, "The influence of measurement noise and electrode mislocalisation on EEG dipole-source localisation," *Med. Biol. Eng. Comput.*, vol. 38, no. 3, pp. 287–296, 2000.
- [6] A. Mitchell and D. Gri ths, *The Finite Difference Method in Partial Differential Equations*. John Willey and Sons, 1980.
- [7] W. H. Press, S. A. Teukolsky, W. T. Vetterling, and B. P. Flannery, *Numerical Recipes in C*. Cambridge University Press, 1995.
- [8] B. Vanrumste, G. Van Hoey, P. Boon, M. D'Havé, and I. Lemahieu, "Inverse calculations in EEG source analysis applying the finite difference method, reciprocity and lead fields," in *Proceedings of the 20th Annual International Conference of the IEEE Engineering in Medicine and Biology Society*, pp. 2112–2115, 1998.
- [9] P. Laarne, J. Hyttinen, S. Dodel, J. Malmivuo, and H. Eskola, "Accuracy of two dipolar inverse algorithms applying reciprocity for forward calculation," *Computers and Biomedical Research*, vol. 33, no. 3, pp. 172–185, 2000.
- [10] J. Sarvas, "Basic mathematical and electromagnetic concepts of the biomagnetic inverse problem," *Phys. Med. Biol.*, vol. 32, no. 1, pp. 11–22, 1987.
- [11] M. S. Hämäläinen, R. Hari, R. J. Ilmoniemi, J. Knuutila, and O. V. Lounasmaa, "Magnetoencephalography-theory, instrumentation, and applications to noninvasive studies of the working human brain," *Reviews of Modern Physics*, vol. 65, no. 2, pp. 413–497, 1993.